https://doi.org/10.5194/egusphere-2026-3988
Preprint. Discussion started: 15 July 2026

European seasonal temperature change since the Last Glacial Maximum from climate models

Gabriel Fénisse[1*], Aurélien Quiquet[2,3], Masa Kageyama[2,3], Pierre-Henri Blard[1,4], David Vincent Bekaert[1]

1. *Centre de Recherches Pétrographiques et Géochimiques UMR 7358, 15 Rue Notre Dame des Pauvres, 54 500 Vandoeuvre-lès Nancy, France*
2. *Laboratoire des Sciences du Climat et de l'Environnement (LSCE), CEA, CNRS, UVSQ, Université Paris-Saclay, Gif-sur-Yvette, France*
3. *Institut Pierre-Simon Laplace (IPSL), Université Versailles Saint-Quentin, Guyancourt, France*
4. *Laboratoire de Glaciologie, Département de Géosciences, Environnement et Société, ULB, Brussels, Belgium*

----

*Corresponding author.
E-mail address: gabriel.fenisse@univ-lorraine.fr (Gabriel Fénisse).

https://doi.org/10.5194/egusphere-2026-3988
Preprint. Discussion started: 15 July 2026

Abstract

The Last Glacial Maximum (LGM, ~21 ka BP) is a key period for evaluating General Circulation Models (GCMs) used for future climate projections. Determining whether regional cooling reflects a uniform decrease in monthly temperatures throughout the year (i.e., no change in temperature seasonality) or a change in temperature seasonality, would have significant implications for many paleotemperature reconstructions, including those based on paleo-glacier equilibrium lines. In this study, we provide an assessment of GCMs as well as iLOVECLIM Earth system model of intermediate complexity downscaled over Europe in terms of temperature seasonality and of its changes at the LGM, compared to the pre-industrial era. Although models show a large dispersion, some common features emerge. The average temperature seasonality decreases from PI to LGM over southern Europe, while it increases further north. Models simulate a slight and consistent increase in seasonality changes along the Atlantic coast, but a larger and more variable increase over eastern Europe. We identify variations in LGM MTCO (mean temperature of the coldest month) as the primary drivers of both temperature seasonality changes and inter-model dispersion in across the GCM and iLOVECLIM outputs, with the largest disagreements occurring in northeastern Europe, over and near the Fennoscandian ice sheet. Motivated by the fact that the iLOVECLIM model produces some features largely different from the GCMs, we perform a series of sensitivity experiments with iLOVECLIM, to understand its different sensitivity to LGM boundary conditions and forcings. These experiments study the sensitivity of the simulated temperature seasonality amplitude to changes in greenhouse gas concentration, thermohaline circulation, albedo and topography of the Fennoscandian ice sheet and vegetation cover. We show that none of these processes, including glacial forcings (inter-model ice sheet extents), explain the observed seasonality change mismatch between iLOVECLM and GCMs. A significant reduction in this mismatch is achieved only by modifying the vertical parametrisation of radiative profiles in iLOVECLIM, suggesting that the lack of an explicit vertical representation of radiative profiles in iLOVECLIM may bias the simulated temperature seasonality changes at the LGM relative to PI. Pollen-based reconstructions are generally consistent with model results. However, the regions that display the largest inter-model differences are also not covered by this type of reconstruction, which is restricted to areas outside the ice sheets. European temperature seasonality since the LGM therefore remains a key yet poorly constrained characteristic of LGM climates, calling for more single-model sensitivity experiments to improve our understanding of past and future temperature seasonality changes.

keywords

Temperature seasonality amplitude; Europe; Last Glacial Maximum compared to present (or pre-industrial); PMIP Global Circulation Models; iLOVECLIM Earth System Model of Intermediate Complexity; Pollen-based data-model comparisons

https://doi.org/10.5194/egusphere-2026-3988
Preprint. Discussion started: 15 July 2026

1. Introduction

The Last Glacial Maximum (LGM, ~21 ka BP) marks the most recent period of near-stable cold climate, providing a benchmark for assessing testing General Circulation Models (GCMs, *Harrison et al., 2015; Kageyama et al., 2017, 2018*). During this period, large-scale continental ice sheets (*Clark and Mix, 2001; Peltier et al., 2004; Tarasov et al., 2002*), low sea level and low greenhouse gas concentration lead to substantially different climate conditions compared to the pre-industrial (PI), making the LGM an ideal test bed for model performance (e.g., *Masson-Delmotte et al., 2006; Ramstein et al., 2007*). Indeed, the wealth of proxy data concerning the climate conditions of this period makes it possible to compare the results of the simulations with paleoclimate archives. For this reason, the Paleoclimate Modelling Intercomparison Project (PMIP; *Joussaume and Taylor, 1995; Joussaume et al., 1999; Braconnot et al., 2012; Kageyama et al., 2018*) has traditionally provided a common modelling framework for LGM climate simulations. However, model simulations exhibit stark inter-model discrepancies in reconstructed LGM cooling, especially in high latitude regions such as Europe (e.g., *Kageyama et al., 2021*). This region also exhibits strong latitudinal and meridional gradients resulting from complex interactions between small spatial scale features (i.e., topography, presence of the Mediterranean Sea) and larger scale circulation (e.g., position of the atmospheric jet (*Beghin et al., 2016*) and Atlantic oceanic circulation) (*Hoar et al., 2004; Kageyama et al., 2021; Russo et al., 2024*). Inter-model discrepancies highlight the need to improve our understanding of regional climate dynamics and underlying mechanisms (e.g., *Lamarque et al., 2013; Beghin et al., 2014; Hernandez et al., 2025*).

Comparing climate simulation outputs with climate reconstructions is a promising approach to isolate local-to-regional climate responses and assess the accuracy of climate simulations. However, multiproxy studies that attempted to reconstruct LGM climate have often faced challenges due to spatial heterogeneity and a lack of robust continental reconstructions (e.g., *Fénisse et al., 2026; Duprat-Oualid et al., 2017; Robles et al., 2023; Davis et al., 2024*). Discrepancies in reconstructed LGM cooling may partly reflect differences in the sensitivity of the indicator to temperature seasonality changes or site-specific conditions. For instance, $\delta^{18}O$ (oxygen isotopic composition) in ice cores and speleothems often captures the signal of the rainy season (*Schlosser and Oerter, 2017; Morgan et al., 2022*), while proxies such as tree rings and pollen may be biased toward growing season climate (*Guiot et al., 1989; Cheddadi et al., 2009*).

Several studies have aimed to quantify temperature seasonality variations during the LGM, using climate simulation outputs (e.g., *Izumi et al., 2013; Pausata et al., 2013; Beghin et al., 2014, 2016*). For example, *Izumi et al. (2013)* investigated temperature seasonality changes as simulated by GCMs for a set of climatic conditions (warm and cold climates, including the LGM). They show that temperature seasonality changes are systematically larger over continents with respect to the ocean, especially in extratropical regions. While proxies such

https://doi.org/10.5194/egusphere-2026-3988
Preprint. Discussion started: 15 July 2026

as pollen data provide quantitative temperature seasonality reconstructions at high spatial resolution and coverage (e.g., *Peyron et al., 1998; Chevalier et al., 2020*), there is no proxy allowing direct reconstruction of LGM temperature seasonality in regions that were ice-covered. Exploring the past response of glaciers and ice sheets to climate forcing has been proposed using models of glacier mass balance (e.g., positive degree-day models (e.g., *Reeh, 1991*)), but these approaches do not allow to reconstruct temperature seasonal variability, nor its fine-scale spatial variations across ice sheets. Consequently, in the current state of knowledge, only climate models provide insights into LGM temperature seasonality over the ice sheets.

In this study, we provide a comprehensive assessment of European temperature seasonality during the LGM, using both PMIP3-CMIP5 and PMIP4-CMIP6 outputs, supplemented by simulations with the Earth system model of intermediate complexity (EMIC) iLOVECLIM, downscaled over Europe. In **Sec. 2**, we present the model database used for this work and the methodology followed for the sensitivity experiments with the iLOVECLIM model. In **Sec. 3**, we discuss the inter-model differences and similarities in terms of temperature seasonality changes. In **Sec. 4**, we evaluate the impact of several physical processes in iLOVECLIM on the simulated temperature change in seasonality at the LGM. Finally, in **Sec. 5** we compare model simulation outputs with proxy-based climate reconstructions from pollen data.

2. Data and methods

2.1 PMIP numerical experiments and database

We analyze climate model outputs from the PMIP3-CMIP5 and PMIP4-CMIP6 ensembles, based on several models listed in ***Table 1***. The forcings and boundary conditions follow the protocols established by PMIP3 (*Otto-Bliesner et al., 2009, Braconnot et al., 2012*, https://wiki.lsce.ipsl.fr/pmip3/doku.php/pmip3:design:21k:final) and PMIP4 (*Kageyama et al., 2017*). In the equilibrium simulations of the LGM, the orbital configuration and the greenhouse gas concentration (*Berger, 1978*) are set to their 21 ka values. Ice sheets are prescribed, but each model adopts different ice sheet extents (ICE-6G_C, *Argus et al., 2014; Peltier et al., 2015* and GLAC-1D, *Tarasov et al., 2012 or the blended PMIP3 product, Abe-Ouchi et al., 2015*). Atmospheric horizontal resolutions and model-specific protocols are also reported in ***Table 1***, which includes information on the output from 18 models. To capture equilibrium climate states and mean temperature seasonality cycles, we analyze 50 years of monthly surface air temperature (*tas*) outputs interpolated on a common 0.25°×0.25° grid covering Europe (35°N-70°N and 10°W-50°E) using a near-neighbour algorithm. The temperature seasonality (S, in °C, ***Eq.1***) is defined as the difference between the mean temperature of the warmest month (MTWA) and the mean temperature of the coldest month (MTCO), for both the LGM and PI simulated climates.

https://doi.org/10.5194/egusphere-2026-3988
Preprint. Discussion started: 15 July 2026

$$S = MTWA - MTCO \quad (1)$$

Temperature seasonality changes between the LGM and PI periods ($\Delta S_{LGM\text{-}PI}$, ***Eq.2***) are defined as:

$$\Delta S_{LGM\text{-}PI} = S_{LGM} - S_{PI} = (MTWA - MTCO)_{LGM} - (MTWA - MTCO)_{PI} \quad (2)$$

This metric measured shifts in seasonal temperature amplitude and identifies regions with possible glacial–interglacial changes in the seasonal cycle. We computed these temperature seasonality changes (LGM–PI) exclusively over present-day continental areas; oceanic regions are therefore not considered in this study.

https://doi.org/10.5194/egusphere-2026-3988
Preprint. Discussion started: 15 July 2026

Model	*Equilibrium Climate Sensitivity (ECS)*	*Prescribed ice sheet reconstruction*	*PMIP/CMIP and rip(f) identifier if several simulations are available*	*Atmosphere resolution (lon × lat)*	*Reference(s)*
AWIESM1	3.6	PMIP4	PMIP4-CMIP6	1.9°× 1.9°	*Sidorenko et al., (2015)* *Lohmann et al., (2020)*
AWIESM2	3.6	PMIP4	PMIP4-CMIP6	1.9°× 1.9°	*Sidorenko et al., (2015)*
CCSM4 (NCAR)	2.9	PMIP3	PMIP3-CMIP5 r2i1p1	1.25°× 0.9°	*Gent et al., (2011)*
CCSM4-UofT	3.2	ICE-6G_C	PMIP4-CMIP6	1.25°× 0.9°	*Peltier and Vettoretti, (2014)* *Chandan and Peltier, (2017)*
CESM1-2	3.6	PMIP4	PMIP4-CMIP6	2.5°× 1.9°	*Tierney et al., (2020)*
CESM2-1	5.3	PMIP4	PMIP4-CMIP6	1.25°× 0.9°	*Zhu et al., (2022)*
FGOALS-g2 (LASG-CESS)	4.4	PMIP3	PMIP3 r1i1p1	2.8°× 3.0°	*Zheng et al., (2013)*
HadCM3-GLAC1D	2.7	PMIP4	PMIP4-CMIP6	3.8°× 2.5°	*Valdes et al., (2017)*
HadCM3-ICE6GC	2.7	PMIP4	PMIP4-CMIP6	3.8°× 2.5°	*Valdes et al., (2017)*
HadCM3-PMIP3	2.7	PMIP3	PMIP4-CMIP6	3.8°× 2.5°	*Valdes et al., (2017)*
INM-CM4-8	2.1	ICE-6G_C	PMIP4-CMIP6-r1i1p1f1	2.0°× 1.5°	*Volodin et al., (2018)*
IPSLCM5A2	-	ICE-6G_C	PMIP4-CMIP6	3.8°× 1.9°	*Sepulchre et al., (2020)*
MIROC-ES2L	2.7	ICE-6G_C	PMIP4-CMIP6 r1i1p1f2	2.8°× 2.8°	*Ohgaito et al., (2021)* *Hajima et al., (2020)*
MPI-ESM-P1	3.5	PMIP3	PMIP3-CMIP5	1.9°× 1.9°	*Giorgetta et al., (2013)*
MPI-ESM1-2	2.8	ICE-6C_C	PMIP4-CMIP6 r1i1p1f1	1.9°× 1.9°	*Maurisen et al., (2019)*
MRI-CGCM3	2.6	PMIP3	PMIP3-CMIP5 r1i1p1	1.1°× 1.1°	*Yukimoto et al., (2012)*
iLOVECLIM GLAC-1D	3.2	GLAC-1D ICE-6G_C	PMIP4	1.25°×0.9°	*Lhardy et al., (2021)*
iLOVECLIM ICE-6G_C	3.2	ICE-6G_C	PMIP4	1.25°×0.9°	*Lhardy et al., (2021)*

Table 1. *Descriptions of the PMIP3 and PMIP4 climate models analyzed in this study.*

https://doi.org/10.5194/egusphere-2026-3988
Preprint. Discussion started: 15 July 2026

2.2 iLOVECLIM model and downscaling approach

In addition to the model outputs present in **Sec. 2.1**, we performed numerical experiments with the Earth system model of intermediate complexity (EMIC) iLOVECLIM (*version 1.1*, *Roche et al., 2014*). Compared to GCMs, EMICs generally have a coarser spatial resolution and/or a simplified representation of physical mechanisms, allowing for a much lower computational cost compared to GCMs. They are particularly suited for climate studies that require long model integrations, such as those exploring equilibrium climate sensitivity (e.g., *Loutre et al., 2004*), ice sheet dynamics (e.g., *Goelzer et al., 2016*), carbon cycle processes (e.g., *Bouttes et al., 2011*), or rapid climate feedbacks occurring in slowly changing orbital forcing (e.g., *Calov et al., 2005*).

The iLOVECLIM model derives from the initial version of *Goosse et al. (2010)*, with which it shares three major components: the ECBilt atmospheric model (*Opsteegh et al., 1998*), a sea-ice and ocean module (*Renssen et al., 2009*), and the VECODE terrestrial vegetation model (*Brovkin et al., 1997*) including three Plant Functional Types (PFTs). Several modules have been added since *Goosse et al. (2010)* to expand represented climate processes, including an oceanic carbon cycle component (*Bouttes et al., 2015*) and an interactive ice sheet model (*Roche et al., 2014*). Here we benefited from the interactive dynamical downscaling embedded in iLOVECLIM (*Quiquet et al., 2018*), which computes a surface air temperature (*tas*) on a fine spatial grid from the model variables available on the coarse native T21 grid (roughly 5.6°, so ca. 550 km). This dynamical downscaling significantly enhances spatial variability at high-resolution (*Arthur et al., 2022, 2025*), allowing for improved comparability of climate model outputs (downscaling grid, ***Fig.S1***) with peloclimate reconstructions (*Zapolska et al., 2023*). Here we apply the downscaling to the 0.25° × 0.25° grid covering Europe used in *Arthur et al. (2022)*. Our reference climate simulation is a long climatic equilibrium (5,000 modeled years) under prescribed boundary conditions and forcings following the PMIP protocols (PMIP3/4). The ice sheets on the coarse iLOVECLIM grid are prescribed following the GLAC-1D reconstructions of *Tarasov et al., (2012)*. For the European sub-grid, GLAC-1D is also used for the Fennoscandian ice sheet, and we also introduce the Alpine (*Seguinot et al., 2018*) and Vosgian (*Harmand et al., 2015*) ice fields reconstructions. The last 100 yr mean climate of these simulations was used for the analysis of temperature seasonality changes.

Two earlier versions of iLOVECLIM contributed to the last PMIP4 exercise and are therefore listed in ***Table 1***. Our simulations differ from these earlier simulations since they activate the interactive dynamical downscaling over Europe, which induces changes in the simulated climate through differences in energy and hydrology budgets. Except for the use of the downscaling, our reference experiment uses the same parameter values as the iLOVECLIM experiment (GLAC-1D ice sheet reconstruction) reported in *Kageyama et al. (2021)*.

https://doi.org/10.5194/egusphere-2026-3988
Preprint. Discussion started: 15 July 2026

2.3 Sensitivity experiments with the iLOVECLIM model

We performed a series of sensitivity experiments to assess the importance of some processes on the simulated temperature seasonality. These experiments are branched from our long-term reference equilibrium LGM simulation presented in **Sec. 2.2**. They are designed so that they only affect the LGM results. As such, temperature changes in seasonality (LGM vs. PI) in each specific sensitivity experiment are compared using the same iLOVECLIM reference provided in this study. The various experiments are summarized in ***Table 2*** and are further described below:

Climate sensitivity. The equilibrium climate sensitivity (ECS) is defined as the degree of warming reached at equilibrium for a doubling of the preindustrial pCO_2 (280 ppm) (*Hansen et al., 1984*). iLOVECLIM shows a low ECS when compared to the PMIP-participating models (***Table 1***). Following *Timm and Timmermann, (2007)*, we artificially increased this ECS multiplying by 1.5 the longwave radiation absorption by CO_2 (ECS=4.8). With this experiment, we aim to evaluate the impact of LGM cooling on European temperature seasonality under enhanced ECS.

Ocean circulation. The velocity and southward shift of North Atlantic Ocean convection associated with the Atlantic Meridional Overturning Circulation (AMOC) strongly influence the position of atmospheric centers of action, such as the North Atlantic jet stream (*Ullman et al., 2014*), which may have varied between the LGM and today. A weakened AMOC can significantly alter heat transport across the North Atlantic, thereby modifying the meridional temperature gradient and the structure of atmospheric circulation cells (*Orbe et al., 2023*). In addition, several studies have highlighted the key role of surface ocean conditions (i.e., sea surface temperatures; SSTs) in modulating AMOC variability and atmospheric circulation, with potential downstream influences on the North Atlantic Oscillation (NAO) and continental climates (*Deser et al., 2000*). For these reasons, we perform two sensitivity experiments in which we artificially alter the simulated oceanic circulation. In one experiment, we impose an important freshwater flux of 0.2 Sv (1 Sv = 10^6 $m^3.s^{-1}$) over the North Atlantic, leading to a complete shutdown of the AMOC. In the other experiment, we favour dense water formation in Antarctica by activating the Antarctic brine sinking mechanism used in *Bouttes et al., 2010, 2023*. In this experiment, the Antarctic bottom water expands northward, resulting in a much shallower upper cell of the AMOC (***Fig.S2***).

Ice sheet effects. Several studies have documented the role of ice sheet forcing during the LGM on atmospheric circulation patterns (e.g., *Kageyama et al., 1999, 2001; Li and Battisti, 2008; Laîné et al., 2009; Pausata et al., 2011; Beghin et al., 2014*). The LGM climate was most likely impacted by the presence of the Fennoscandien ice sheet (*Rørvik et al., 2010*) through both thermal forcing (due to albedo and related temperature changes) and orographic forcing (due to elevation on temperature and circulation pattern). To assess the influence of the ice sheet on European climates, we perform two sensitivity experiments: (i) a “flat ice sheet”

https://doi.org/10.5194/egusphere-2026-3988
Preprint. Discussion started: 15 July 2026

simulation, where we assign the PI topography to the area covered by the Fennoscandian ice sheet under LGM conditions while keeping the LGM ice mask (high albedo), and (ii) a "dark ice sheet" scenario, where we use the LGM topography but no longer apply the icemask, such that the albedo in summer eventually reduces to bare soil albedo. These modifications are only applied in the region impacted by the downscaling (***Fig. S1***).

Vegetation model. Vegetation-driven biogeophysical feedbacks (e.g., taiga–tundra transitions) contributed significantly to LGM climate cooling (up to –2°C) in northern latitudes (*Jahn et al., 2005*), potentially surpassing the radiative impact of reduced atmospheric CO_2 in these regions. In order to assess the impact of vegetation changes on temperature seasonality, we performed an experiment in which we prescribed the PI vegetation cover to the LGM simulation.

Atmospheric radiative code. In order to reduce the computational cost, the atmospheric component of the iLOVECLIM model (ECBilt) has a very simple vertical representation. Notably, due to the lack of an explicit representation of some vertical processes, the radiative scheme uses imposed vertical profiles of temperature, humidity, and ozone to compute net shortwave radiation from the NCEP/NCAR reanalyses (National Centers for Environmental Prediction and National Center for Atmospheric Research). These profiles are region-specific (e.g., Greenland, high latitudes, North America, etc.; *Opsteegh et al., 1998*). In our reference simulation, all the Northern Hemisphere grid points that change from ice free in the PI run to ice sheet in the LGM run, switch to the Greenland profile instead of their native profile. As such, grid points corresponding to the Eurasian ice sheet make use of the Greenland profile at the LGM and the standard European profile for the PI simulation. In one sensitivity experiment, we evaluated the impact of this specific model feature on the simulated temperature seasonality by keeping the vertical radiative profile of PI conditions for a LGM simulation.

Sensitivity experiment	***Feature***
ECS	Increased sensitivity to CO_2 change
BRINES	Shallower AMOC upper branch
FWF	AMOC shutdown
DarkIS	Modified fennoscandian ice sheet LGM topo but PI icemask
FlatIS	Modified Fennoscandian ice sheet PI topo but LGM icemask
FixVEG	Interactive vegetation not activated (prescribed to PI values)
IRN	No change in the radiative vertical profiles at the LGM with respect to PI

https://doi.org/10.5194/egusphere-2026-3988
Preprint. Discussion started: 15 July 2026

Table 2. *Sensitivity experiments branched from the reference long-equilibrium simulation.*

3. Monthly outputs from PMIP3/PMIP4 and iLOVECLIM models

3.1 European temperature seasonality changes

Fig.1 provides a synthesis of European temperature seasonality changes (i.e. LGM - PI difference) extracted from the models listed in ***Table 1*** (both GCMs and iLOVECLIM) and from our reference LGM iLOVECLIM configuration (**Sec. 2.2**). All model outputs are interpolated onto the same European 0.25°x0.25° grid using the same method (nearest neighbour) as the one embedded in iLOVECLIM. ***Fig.1*** also shows the multi-model mean. Most models show an increase in temperature seasonality amplitude during the LGM compared to PI conditions (i.e., positive temperature seasonality changes; ***Equ.2***) in continental Europe, especially towards the East of our domain. However, there are large inter-model differences. For instance, the iLOVECLIM models produce a reduced temperature seasonality (from -5°C to -15°C) in the easternmost regions, while CESM1.2 shows an increase in temperature seasonality larger than +30°C in the vicinity of the Fennoscandian ice sheet. However, most models produce an increase in temperature seasonality smaller than 20°C and iLOVECLIM is the only model that produces a decreased temperature seasonality in the vicinity of the ice sheet. In contrast to eastern Europe, the coastal southern regions show a reduced temperature seasonality at the LGM compared to PI, especially in the Iberian Peninsula. The models show a relatively good agreement on this feature, with a reduced temperature seasonality at the LGM by -5°C to -10°C.

Finally, ice-covered regions display significant inter-model differences, with either a decrease or an increase of temperature seasonality at the LGM compared to PI (***Fig.1***). For instance, the three iLOVECLIM models produce a strongly reduced LGM temperature seasonality, by as much as 20°C. A reduced LGM temperature seasonality, although less pronounced, is also suggested by several GCMs (FGOALS-g2, IPSL-CM5-A2, AWI-ESM-2, MPI-ESM1-2). On the other side of the spectrum, CESM2-1 produces a large increase in temperature seasonality, reaching more than +20°C). Some models also support an increased LGM temperature seasonality (CCSM4, INM-CM4.8, MIROC-ES2L, MRI-CGCM3), although to a much smaller extent. ***Fig.S1*** provides the individual mean temperature seasonal cycles onto the European downscaling grid.

https://doi.org/10.5194/egusphere-2026-3988
Preprint. Discussion started: 15 July 2026

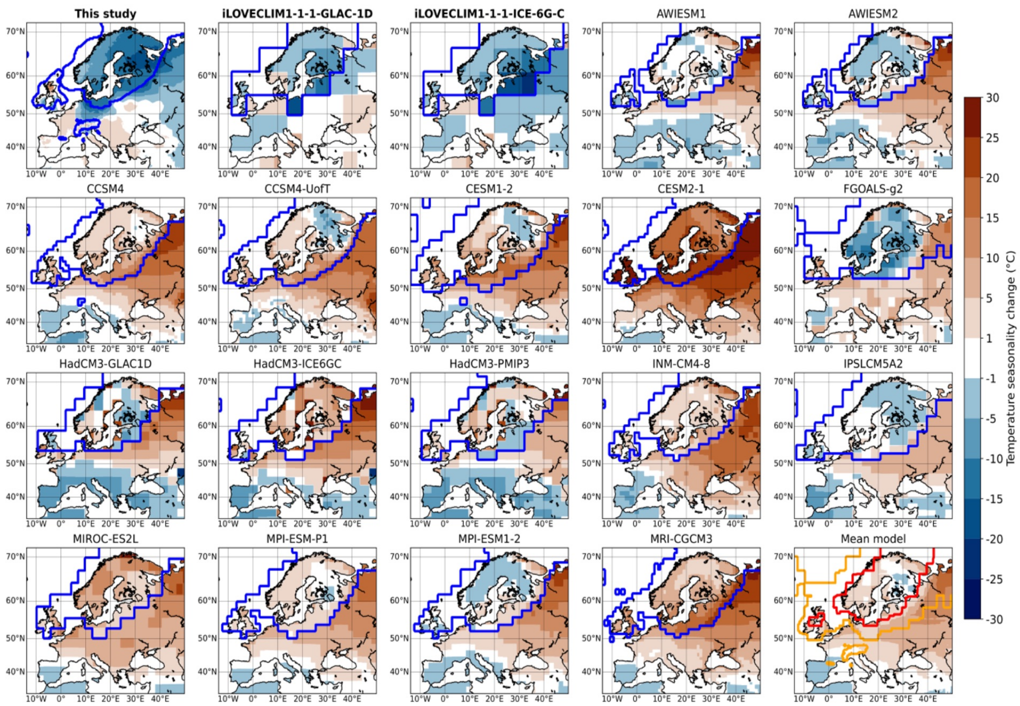

Figure 1. *Continental* temperature *seasonality anomaly (i.e.,* $\Delta S_{LGM\text{-}PI}$ *from* ***Equ.2****) simulated by each climate model (PMIP3 and PMIP4 ensembles and iLOVECLIM reference model) and their respective ice masks in the European area (blue). Climate models results are downscaled on the same grid (0.25°×0.25°) with the nearest interpolation method. The multi-model mean is shown at the bottom right with the label "Mean Model". Names in bold refer to iLOVECLIM simulations. Red and orange contour lines indicate the common and maximum ice sheet extents, respectively, among all models, including GCMs and iLOVECLIM.*

Fig.2a shows the temperature annual cycle, averaged over the continents, simulated for the LGM by each model. The inter-model spread quantifies: ~10°C in summer and ~20°C in winter. LGM cooling from individual models are reported in ***Fig.S3***. CESM2.1 simulates a systematically colder climate than the multi-model mean by about 10°C. iLOVECLIM produces the warmest summer in its downscaled version and the warmest winter in its not downscaled version. The change in monthly temperature at the LGM compared to PI is depicted in ***Fig.2b***. While some models show a drastic winter cooling and moderate summer changes (e.g., CESM2-1), this feature stands out as it displays a behavior that is clearly distinct from all other models.

https://doi.org/10.5194/egusphere-2026-3988
Preprint. Discussion started: 15 July 2026

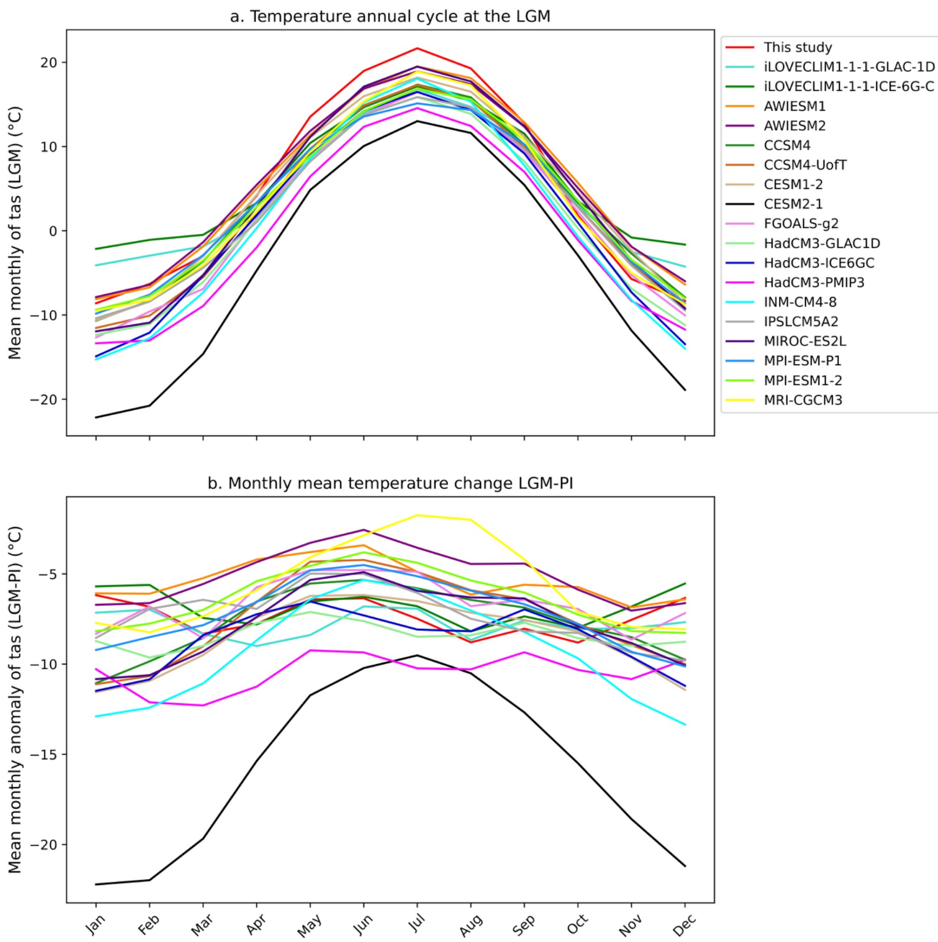

Figure 2. *Mean continental (including ice sheet) temperature seasonal cycles interpolated onto the European downscaling grid during the LGM **(a)** and LGM–PI **(b)**, derived from iLOVECLIM and GCM outputs (colored lines).*

https://doi.org/10.5194/egusphere-2026-3988
Preprint. Discussion started: 15 July 2026

To further illustrate the inter-model differences, we show in ***Fig.3*** the changes in LGM continental temperature seasonality (ΔS_{LGM-PI} *from* ***Equ.2***) expressed as a zonal mean (***Fig.3a***) and as a meridional mean (***Fig.3b***) These means include all continental grid boxes, ice-covered and ice-free. Differences between profiles may partly reflect the contrasts in spatial resolution among models.

The models all produce weak changes in temperature seasonality at low latitudes of the European domain (from -3 to -6°C south of 35°N, ***Fig.3a***), over Southern Europe. All models simulate an increase in LGM - PI seasonality change towards the North, up to 55°N (***Fig.3a***). However, the magnitude of this increase is model dependent, as well as the value of the maximum seasonality change, which ranges from -3 to 27°C. The spread of model results increases north of 55°N: most GCMs simulate a LGM - PI seasonality increase close to its maximum around 55°N (+10°C on average), whereas the three iLOVECLIM simulations indicate a reduction in LGM temperature seasonality (-5°C on average) north of 50°N. The resulting multi-model mean ("Mean Model", pink line in ***Fig.3***) thus displays positive temperature seasonality changes (+7°C) across high latitudes, becoming particularly pronounced north of 60°N.

The meridional mean (***Fig.3b***) shows a gradual increase in the LGM - PI seasonality change with increasing longitude, except for the iLOVECLIM models which simulate a decreased seasonality from 8°E eastwards (downscaled iLOVECLIM) and from 14°E for the other iLOVECLIM versions. However, the intermodel spread remains slightly smaller than for the zonal mean values shown on ***Fig.3a***.

Although CESM2-1 behaves somewhat as an outlier in its amplitude, its temperature seasonality change patterns still broadly follow the latitudinal and longitudinal trends simulated by most other models.

https://doi.org/10.5194/egusphere-2026-3988
Preprint. Discussion started: 15 July 2026

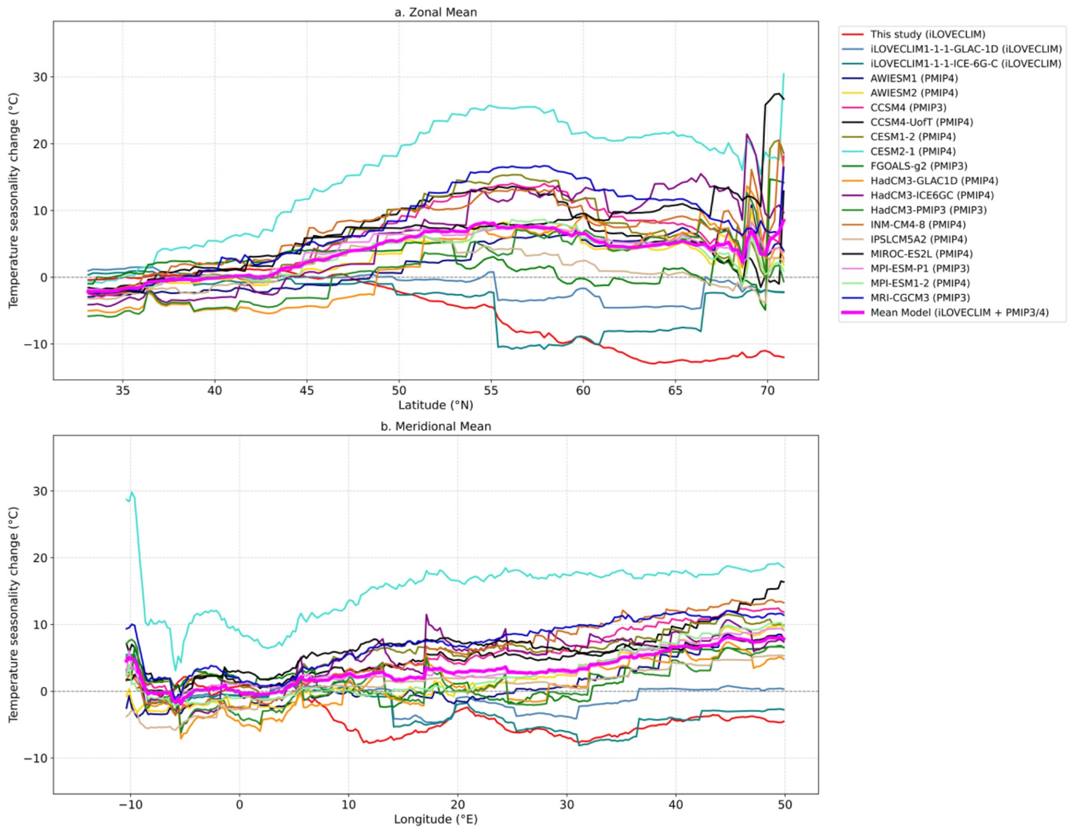

Figure 3. *Zonal **(a)** and meridional **(b)** averages of temperature seasonality mean annual changes (i.e., ΔS_{LGM-PI} from **Equ.2**) simulated by GCMs and iLOVECLIM on continents (including ice sheet covered areas) across Europe* (35°N-30°N and 10°W-50°E).

Since ***Fig.1*** shows a large inter-model spread over the ice sheet, we explore the changes in temperature seasonality for both ice-covered and ice-free model grid points (***Fig.4***). Over ice-free continental areas (black boxes in ***Fig.4***), temperature seasonal changes consistently fall between 0°C and +5°C (only CESM2-1 produces a mean seasonal amplitude increase of +14°C compared to PI). Changes in temperature seasonality over glaciated regions (blue boxes in ***Fig.4***) show larger disparities across models. In short, we observe a continuum of model response from the large reduction in LGM temperature seasonality suggested by the iLOVECLIM models (about -12°C) to the large increase in LGM temperature seasonality simulated by CESM2-1 (up to +18°C).

Some models do not show contrasted responses over ice sheets compared to ice free areas (***Fig.4***). For example, the median value for temperature seasonality change is compatible between these two domains for AWIESM1, CCSM4, CESM1-2 and HadCM3-GLAC1D. Then, half

https://doi.org/10.5194/egusphere-2026-3988
Preprint. Discussion started: 15 July 2026

of the models suggest a reduction of the median value while the other half suggest an increase. The largest differences between ice-free and ice-covered regions is given by our reference iLOVECLIM model (-13°C for ice-covered and near-zero for ice-free) followed by FGOALS-g2 (-7°C for ice-covered and +4°C for ice-free).

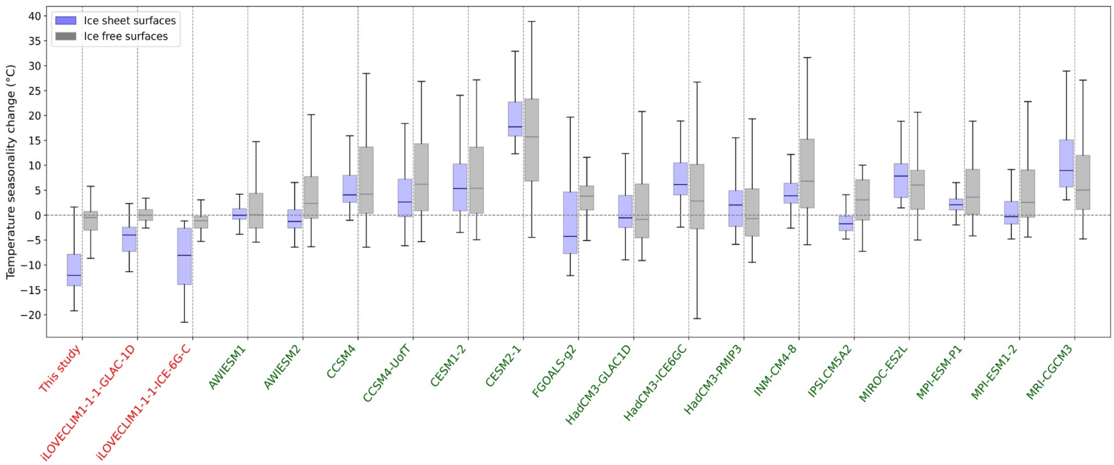

Figure 4. *Mean European temperature seasonality changes (LGM-PI) on ice free (black boxes) and ice-covered (blue boxes) areas, computed to the downscaling grid (* ***Equ.2)****. The boxplots show the median (central line), the interquartile range (box, 25th–75th percentiles), and the whiskers indicating the minimum and maximum values over the given area. X-axis labels are colored red for iLOVECLIM and green for GCM outputs. The mean temperature seasonal cycle is computed over the last 50 years of the simulations for each model.*

3.2 Decomposing temperature seasonality changes into MTCO and MTWA

To understand the origin of the inter-model disparities in temperature seasonality changes, we decompose the terms used in the calculation of the temperature seasonality change (ΔS_{LGM-PI} *from* ***Equ.2***). ***Fig.5*** presents the standard deviations (STD), computed from all models, of the PI and LGM temperature seasonalities, as well as the MTWA and MTCO at the LGM (individual model responses for these variables are shown in ***Figs.S4 and S5***). While PI temperature seasonal amplitudes are generally consistent across models (STD < 2°C on average; ***Fig.5a***), LGM temperature seasonality shows much larger discrepancies (up to 12°C, ***Fig.5b***). These results suggest that the model discrepancies observed in ***Fig.1*** are primarily driven by the simulated LGM climate, with the strongest disagreements (up to 10 °C) located near the Fennoscandian ice sheet.

To further address the origin of these discrepancies in LGM temperature seasonality, we investigate the respective changes in MTWA and MTCO (***Figs.5c*** and ***5d***). LGM MTWA shows relatively good agreement among simulations (STD ≤ 5°C, ***Fig.5c***), where a zone of maximum

https://doi.org/10.5194/egusphere-2026-3988
Preprint. Discussion started: 15 July 2026

variability (STD ≈ 5 °C) is located in the inter–ice-sheet mask area. In contrast, LGM MTCO values display substantial inter-model disagreement among simulations (up to 12°C; ***Fig.5d***). Although the maxima of standard deviation for both MTCO and temperature seasonality are located around the ice sheet, indicating that LGM MTCO is the main contributor to inter-model disagreement in temperature seasonality changes, MTCO changes remain overall more spatially homogeneous than the LGM temperature seasonality pattern (***Fig.5d***).

Finally, iLOVECLIM simulations tend to produce significantly milder winters, with MTCO values on average +10°C to +20°C warmer than those of the GCMs (***Fig.S5***). This feature most likely explains why the change in temperature seasonality simulated by iLOVECLIM at the LGM differs substantially from the rest of the GCMs (e.g., ***Fig.1***).

This different model behaviour in iLOVECLIM calls for further investigation of the physical processes in this particular model, including those related to glacial forcings, which could affect the simulated changes in temperature seasonality since the LGM.

https://doi.org/10.5194/egusphere-2026-3988
Preprint. Discussion started: 15 July 2026

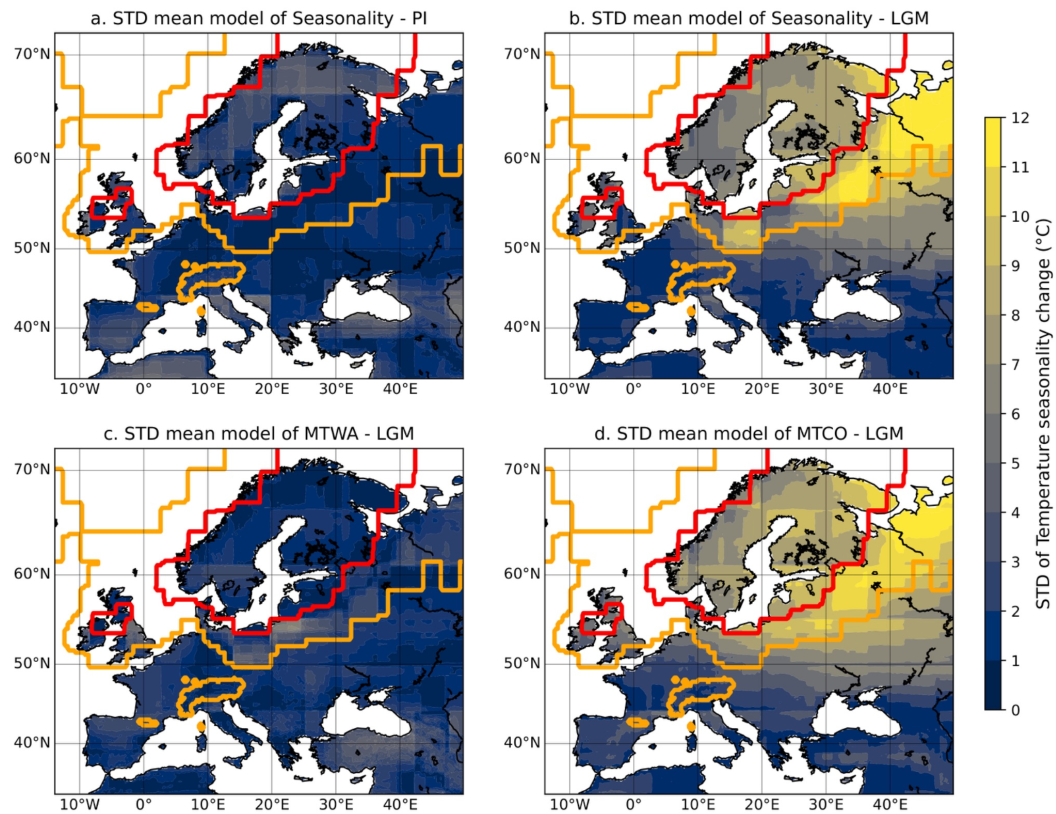

Figure 5. *Standard deviations of temperature seasonality (i.e., S from Equ.1) for PI* ***(a)*** *and LGM conditions* ***(b)****, derived from all models, including GCMs and iLOVECLIM outputs. We also present STD maps of MTWA* ***(c)*** *and MTCO* ***(d)*** *during the LGM. Red and orange contour lines indicate the common and maximum ice sheet extents, respectively, among all models, including GCMs and iLOVECLIM.*

4. Sensitivity experiments to identify the drivers of glacial-interglacial temperature seasonality changes

We have shown in the previous section that temperature seasonality changes are markedly different among models. In particular, iLOVECLIM model temperature seasonality changes at the LGM stand out from most of GCMs, likely explained by the much warmer MTCO at the LGM in this model. In this section, we present iLOVECLIM sensitivity experiments aimed to investigate the impact of different mechanisms and model parametrizations on simulated LGM temperature seasonalities. ***Fig.6*** summarizes the outputs of all the sensitivity

https://doi.org/10.5194/egusphere-2026-3988
Preprint. Discussion started: 15 July 2026

experiments listed in ***Table 2***, reported as changes in MTWA, MTCO and temperature seasonality relative to our reference iLOVECLIM simulation using the downscaled European grid. Absolute changes in temperature seasonality from PI to LGM (i.e., without subtracting it to the reference simulation) are shown in ***Fig.S6***. Below, we describe and discuss each sensitivity test separately, with a focus on the glaciated regions where the strongest discrepancies in temperature seasonal amplitude occur. In order to address the temperature seasonality discrepancies across iLOVECLIM and GCM outputs (***Figs.1, 2 and 3***) in this section, it would be necessary to preserve summer conditions (MTWA) - where models generally agree (***Fig.5c***) - and to identify a process affecting MTCO values, in particular near the ice sheets, in order to improve the consistency between the model outputs during the LGM.

4.1 Impact of ice sheet topography and ice mask

Reducing the ice sheet thickness (hereafter referred to as "FlatIS") down to zero (i.e., pre-industrial ice thickness) yields an increase of winter temperature (MTCO) of +5°C to +15°C over glaciated areas and +1°C to +5°C over ice-free regions (***Fig.6a***). Summer temperature (MTWA) uniformly increases across the continent (from +5°C to +10°C), resulting in relatively small deviations in temperature seasonal amplitude anomalies (from –5°C to +5°C) compared to the reference simulation. The topographic effect (i.e., through lapse rate mechanisms; *Lofverstrom and Liakka, 2018*) thus lowers MTCO (from –5°C to -15°C) more than MTWA (from -5°C to -10°C), but its influence remains minor over ice-free areas. Overall, the temperature seasonality outside of the ice sheet is only marginally (from +1°C to +5°C) affected by changes in the thickness of the ice sheets.

Changes in the albedo of the ice sheet ("DarkIS") produce much stronger increase of MTWA (from +5°C to +20°C) than topography changes ("FlatIS"), without significantly affecting MTCO (from +1°C to -1°C; ***Fig.6b***). This results in a marked flattening of the temperature seasonal cycle over the ice sheet margins and interior, with anomalies reaching +10°C up to +20°C relative to the iLOVECLIM reference simulation, while leaving temperature seasonality of the ice-free areas largely unchanged.

In summary, ice sheet topography and albedo have an impact on the simulated temperature seasonality at the LGM. However, albedo only affects MTWAs, not MTCOs, whereas the major differences observed for iLOVECLIM with respect to the GCMs is on MTCOs. As such, differences in ice sheet extent and albedo in iLOVECLIM are unlikely to explain the differences in simulated temperature seasonality changes at the LGM. In turns, topography does impact the MTCO more than MTWA, with the flat ice sheet experiment producing a flattened temperature seasonal cycle. Since iLOVECLIM already displays a flattened temperature seasonal cycle compared to GCMs (***Fig.1***), this result suggests that an increase of topography could eventually reduce the mismatch between iLOVECLIM and the mean response of the GCMs. However, the flat ice sheet experiment is an extreme case scenario (reduction of more than 2 km of the topography in some places) that produces a

https://doi.org/10.5194/egusphere-2026-3988
Preprint. Discussion started: 15 July 2026

relatively moderate change in seasonality. Overall, ice sheet differences between iLOVECLIM and GCMs are therefore unlikely to explain the observed temperature seasonality change mismatch.

4.2 Impact of increased Equilibrium Climate sensitivity

Amplifying the longwave radiative impact of CO_2 by +50% (which corresponds to an artificial amplification of the ECS) leads to decreased MTCO and MTWA, compared to the iLOVECLIM reference simulation ("ECS", ***Fig.6c***). Increasing this parameter in our iLOVECLIM configuration produces a much colder climate (widespread 15 to 25°C cooling). This decrease is generally more pronounced for the MTWA than for the MTCO, leading to an overall decrease in temperature seasonality (around -10°C in Central and Eastern Europe). Locally, some places can experience an increased temperature seasonality, with for example +5°C in the Iberian Peninsula compared to the iLOVECLIM reference simulation. Nonetheless, the main impact of a greater sensitivity to atmospheric CO_2 concentrations is a flattened temperature seasonal cycle with respect to the reference simulation, caused by a greater change of MTWA compared to MTCO. The MTWA is more strongly affected than MTCO, likely because of the albedo effect. With an increased ECS, we notably simulate a larger extent of perennial snow cover (i.e., snow on ground during summer), particularly in Eastern Europe. An additional mechanism related to albedo is that we simulate a southward shift of the vegetation: tree albedoes are replaced by grass, which further increases the albedo in the ECS experiment with respect to the reference experiment. Since ECS mostly impacts MTWA and not MTCO, the relatively low climate sensitivity of iLOVECLIM is unlikely to explain the temperature seasonality change mismatch with respect to the GCMs.

4.3 Impact of changes in the oceanic circulation

The experiment labeled "FWF" corresponds to a shutdown of the AMOC (through freshwater injection in the North Atlantic). With respect to the reference simulation, this experiment decreases both the MTWA and the MTCO (from -5°C to -20°C), especially in central Europe where temperature anomalies (i.e., MTWA and MTCO) are strongest (***Fig.6d***). The resulting temperature seasonality changes correspond to a flattening of the temperature seasonal cycle by up to +10°C in this area, while the temperature seasonal cycle is almost conserved in the rest of Europe. Thus, "ECS" and "FWF" show a similar model response, i.e., a cooling of both the MTWA and the MTCO, but more pronounced for the MTWA due to albedo changes in a colder climate. As for the "ECS" experiment, a change in the AMOC strength will not allow for a more consistent response of iLOVECLIM with respect to the GCMs.

The second experiment that alters oceanic circulation is the "BRINES" experiment, in which 60% of the salt rejection due to sea ice formation in the Austral Ocean is transferred to the bottom cell of the ocean. This leads to a shallower AMOC upper cell (***Fig.S2***). This experiment ("BRINES") yields only minimal impact on the temperature seasonal

https://doi.org/10.5194/egusphere-2026-3988
Preprint. Discussion started: 15 July 2026

cycle compared to the reference experiment (***Fig.6e***). It mainly impacts the areas covered by the Fennoscandian ice sheet, slightly flattening (by ~+5°C) the temperature seasonal amplitude due to a modest MTCO change relative to the reference simulation. MTWA values over Europe are not significantly affected by the brines experiment (+1°C to -1°C, ***Fig.6e***). While this sensitivity experiment might produce a more realistic LGM oceanic circulation (*Bouttes et al., 2010*), the change in simulated temperature seasonality at the LGM is weak and does not produce results more consistent with the rest of the GCMs.

4.4 Impact of vegetation changes

The “FixVege” experiment corresponds to a simulation in which the LGM vegetation remains at its PI condition. This experiment only has a limited impact on the temperature seasonal differences with respect to the reference LGM experiment (“FixVege”, ***Fig.6f***). By retaining PI vegetation in the LGM configuration, vegetation changes induce comparable MTWA and MTCO warmings across Europe (by +1 °C to +5 °C) relative to the iLOVECLIM reference simulation. This is explained by the fact that the PI vegetation has a greater fraction of trees with respect to grass, and the presence of trees reduces the albedo. Overall, we observe slightly positive temperature seasonal amplitude anomalies in Central Europe, and values close to zero elsewhere, again suggesting a limited contribution of vegetation to LGM temperature seasonality patterns over Europe. This process is therefore also unable to explain the mismatch between iLOVECLIM and the GCMs.

4.5 Impact of the imposed vertical radiative profile

The experiment with an altered vertical radiative profile over the ice sheet (“IRN”) shows MTWA values that are globally preserved, between -2 °C and +2 °C compared to the iLOVECLIM reference simulation (***Fig.6g***). In turns, MTCO decreases by +5°C to +15 °C, especially in ice sheet margin areas like Eastern Europe. The simulated temperature seasonality is thus increased with respect to the reference experiment, meaning that the LGM temperature seasonal cycle is amplified compared to PI conditions. We showed in **Sec. 3.1** (***Figs.1, 2 and 3***) that in Eastern Europe, the iLOVECLIM reference experiment fails to reproduce the increase in temperature seasonality at the LGM with respect to PI simulated by the GCMs. The “IRN” experiment appears to reduce this mismatch in this region.

Among the sensitivity tests performed in this study, the “IRN” experiment is the only one that is able to reduce the mismatch between iLOVECLIM and the GCMs. For this reason, we show in ***Fig.7*** the differences between the simulated temperature seasonality change at the LGM in iLOVECLIM relative to the multi-model mean of the GCMs, for the reference simulation (***Fig.7a***) and for the “IRN” experiment (***Fig.7b***). The dispersion with the GCMs is reduced in Eastern Europe in the “IRN” experiment, especially in the vicinity of the ice sheet. Conversely, the inter-model dispersion is increased in Southern regions.

https://doi.org/10.5194/egusphere-2026-3988
Preprint. Discussion started: 15 July 2026

To summarize, the "IRN" experiment highlights the critical role of the imposed vertical profiles in iLOVECLIM in the simulated temperature seasonality change at the LGM. This reveals a structural limitation stemming from the model's lack of explicit vertical representation.

https://doi.org/10.5194/egusphere-2026-3988
Preprint. Discussion started: 15 July 2026

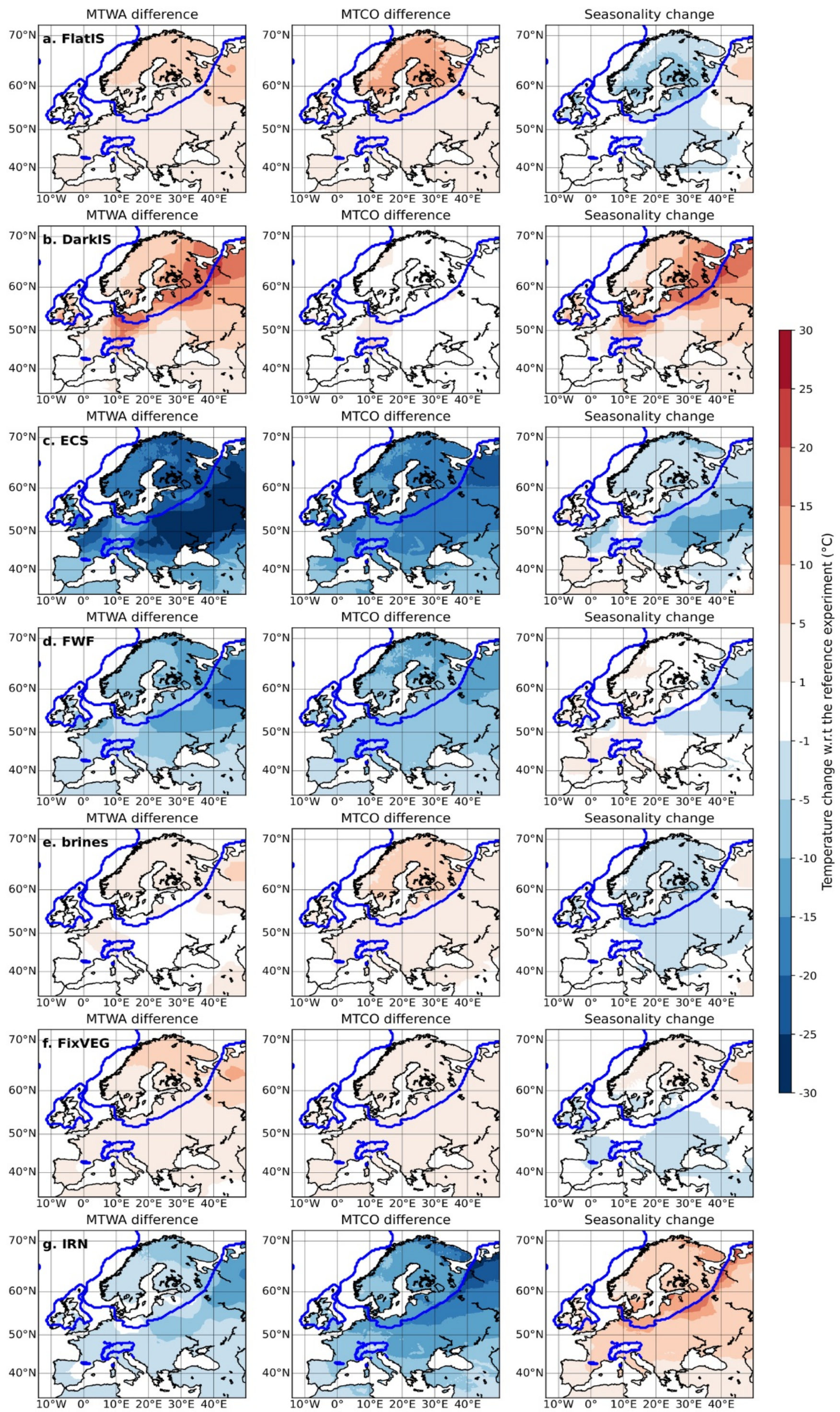

https://doi.org/10.5194/egusphere-2026-3988
Preprint. Discussion started: 15 July 2026

*Figure 6. Impact of the tested process with respect to the reference iLOVECLIM experiment (Test results - reference) on the LGM simulated MTWA (**a**), MTCO (**b**) and temperature seasonality (**c**, i.e. a-b). The names of experiments are reported in **Table 2**. FIS stands for Fennoscandian ice sheet.*

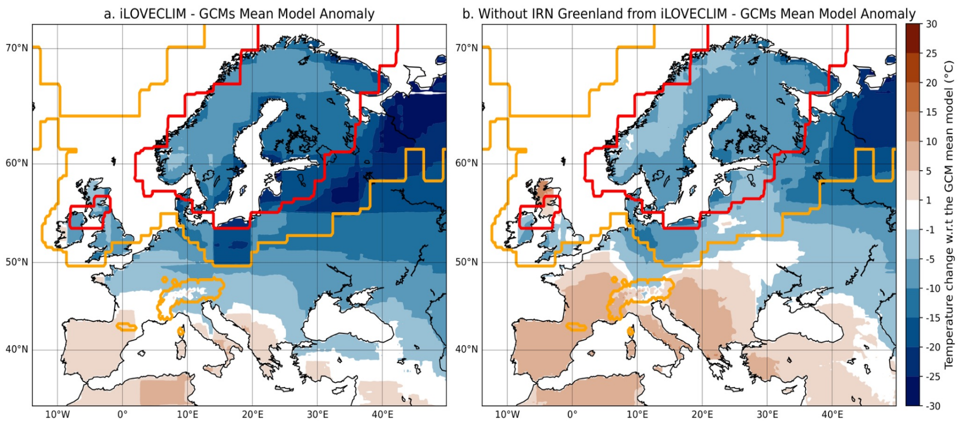

***Figure 7.** Difference in the simulated temperature seasonal change (LGM-PI, ΔS_{LGM-PI} from **Equ.2**) between iLOVECLIM and GCM multi-model means: for the reference experiment **(a)**, and for the "IRN" experiment **(b)**. Red and orange contour lines indicate the common and maximum ice sheet extents, respectively, among all models, including GCMs and iLOVECLIM.*

5. Comparison with pollen-based climate reconstruction

Simulated changes of LGM seasonality in the multi-model mean (including the iLOVECLIM reference experiment and the GCMs) are shown in ***Fig.8*** and compared with pollen-based reconstructions from *Fénisse et al., 2026*. These authors followed a multi-method approach that combines statistical and probabilistic techniques to provide quantitative reconstructions of LGM cooling and temperature seasonality anomalies across Europe. The comparison between model outputs and pollen data provides a way to independently assess the validity of the simulation outputs, although one should bear in mind the potential limitations of the data in documenting LGM temperature seasonality (e.g., *Rehfeld et al., 2016*).

In Europe, pollen-based temperature seasonal climate reconstructions range from -8°C to +8°C (***Figs 8a***). Although some pollen-based temperature seasonal changes range from +8 °C near the coasts to -8 °C inland, pollen-based climate reconstructions do not clearly exhibit well-defined spatial gradients, in contrast to the pronounced temperature seasonal gradients seen in the models (***Fig. 8a–b***). In northern Europe, two data points near the edge of the Fennoscandian ice sheet show contrasting temperature seasonal changes of +1 °C and +4 °C, consistent with mean model simulations, which suggest a +4 °C temperature seasonal

https://doi.org/10.5194/egusphere-2026-3988
Preprint. Discussion started: 15 July 2026

amplification (***Fig.8a***). We note also that for some models the ice mask covers the location of pollen-based reconstructions, complicating data-model comparison.

Unfortunately, climate reconstructions from pollen data do not cover the regions of highest inter-model disagreement (***Fig.8b***, including glaciated areas of the ice sheets), particularly in Central and Eastern Europe, making data–model comparison of LGM temperature seasonality in this part of Europe challenging. These results show that pollen-based reconstructions do not allow discrimination between the models.

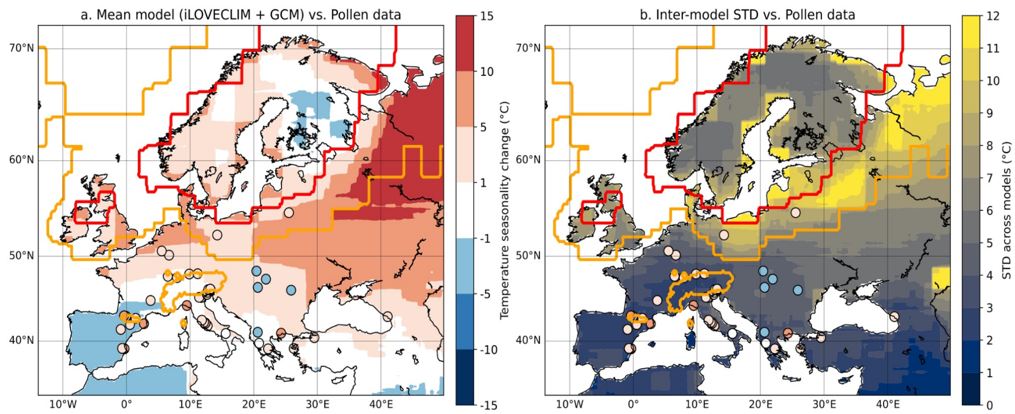

Figure 8. *Continental temperature seasonality change (LGM–PI, ΔSLGM–PI from* ***Equ.2****) derived from pollen-based reconstructions using multi-method approach (Fénisse et al., 2026), compared to* ***(a)*** *mean models (iLOVECLIM and GCMs) and* ***(b)*** *inter-model standard deviation (STD from iLOVECLIM and GCMs) across the downscaled European grid. Temperature seasonality changes from pollen data points are shown in* ***(b)****. Red and orange contour lines indicate the common and maximum ice sheet extents, respectively, among all models, including GCMs and iLOVECLIM.*

5. Conclusions and perspectives

This study presents a climate model compilation, including PMIP and iLOVECLIM simulations, exploring European temperature seasonality during the Last Glacial Maximum (LGM). Our comparison of downscaled iLOVECLIM simulations with GCMs outputs from PMIP3-CMIP5 and PMIP4-CMIP6 models reveals stark inconsistencies in temperature seasonal changes from LGM to PI, including over glaciated Fennoscandian regions. Seasonality anomalies vary across GCMs, but they exhibit common spatial patterns that differ from those simulated by iLOVECLIM. However, we globally show that the temperature seasonality changes from iLOVECLIM and GCMs reproduce the latitudinal and continental gradients, as well as the influence of ice sheet proximity on temperature seasonality changes. By comparing MTCO and MTWA LGM-PI variations, we show that inter-model temperature seasonal dispersions are primarily driven by simulated LGM MTCO over Fennoscandien ice sheet

https://doi.org/10.5194/egusphere-2026-3988
Preprint. Discussion started: 15 July 2026

regions. This result would have significant implications for the annual LGM cooling estimated from paleo-ELA, since glacier modeling requires strong assumptions on temperature seasonality (e.g., PDD method, *Heyman et al., 2013; Blard et al., in prep.*).

To investigate iLOVECLIM's substantial differences from the GCMs, we performed iLOVECLIM sensitivity experiments involving modification of key processes and model parameters on LGM temperature seasonalities from iLOVECLIM. With the exception of experiments that do not impact LGM temperature seasonality, most simulations tend to show a preferential reduction in MTWA compared to MTCO, primarily driven by summer albedo effects. Moreover, these processes produce large-scale responses rather than changes confined to the high-variability region of northern Europe, adjacent to the Fennoscandian ice sheet. Thus, most sensitivity experiments fail to account for the inter-model variability in LGM temperature seasonality. Only by modifying the vertical radiative scheme used in iLOVECLIM were we able to reduce this mismatch in seasonal anomalies between iLOVECLIM and the GCMs. This suggests that the absence of an explicit vertical radiative representation of iLOVECLIM contributes to making this model different from the other ones in terms of LGM-PI temperature seasonality changes.

The reconstructed temperature seasonal changes based on pollen data (*Fénisse et al., 2026*) are spatially variable and do not document the regions of strongest inter-model temperature seasonality disagreement near the Fennoscandian ice sheet. Further clarifying the drivers of glacial temperature seasonality change and inter-model spread represents a pathway toward improving paleoclimate simulations and reducing uncertainties in future climate projections.

Since we show that albedo changes from glacial forcings explain a large part of the simulated change in temperature seasonality, future research could focus on better quantifying land surface feedback, especially over ice sheet regions. Such a process, particularly along the margins of the Fennoscandian ice sheet in Eastern Europe, could help explain the persistent temperature seasonality disagreements between climate models. Finally, a systematic multi-proxy evaluation of LGM winter temperatures at the regional scale is needed to better constrain inter-model variability and improve the consistency of paleoclimate reconstructions across Europe. Precipitation also appears to be a complex yet potentially key variable for studying future temperature changes in the framework of past, on-going and future climate changes.

https://doi.org/10.5194/egusphere-2026-3988
Preprint. Discussion started: 15 July 2026

Data availability

All mean temperature seasonality cycles of the climate models are available in **Supplementary Materials 1**. The data used in this paper are summarized in this repository.

Fénisse, G., Quiquet, A., Kageyama, M., Blard, P.-H., & Bekaert, D. V. (2026). Supplementary materials for the article (CP) "European seasonal temperature change since the Last Glacial Maximum from climate models". Zenodo. https://doi.org/10.5281/zenodo.21159688

The results from the PMIP3-CMIP5 and PMIP4-CMIP6 models can be downloaded on the ESGF (Earth System Grid Federation) website.

Scientific contributions - Authorship contribution statement

Role of each author: Fénisse G., Quiquet A., Kageyama M., Blard P.-H. and Bekaert D.V. designed the study. Fénisse G. and Quiquet A. conceived and ran the iLOVECLIM model experiments. All co-authors discussed the results. Fénisse G. wrote the manuscript with inputs from all co-authors.

Acknowledgements

This study is financially supported by the ANR (ANR-22-CPJ2-0005-24/39 584 01, awarded to D.V. Bekaert). The project is supervised by Aurélien Quiquet (CNRS, LSCE/IPSL, CEA-CNRS-UVSQ) and Pierre-Henri Blard (CNRS–CRPG), David Bekaert (CPJ, Université de Lorraine – CRPG); with the external collaboration of Masa Kageyama (CNRS, LSCE/IPSL, CEA-CNRS-UVSQ). A. Quiquet acknowledges funding from Agence Nationale de la Recherche – France 2030 as part of the PEPR TRACCS programme under grant number ANR-22-EXTR-0010.

https://doi.org/10.5194/egusphere-2026-3988
Preprint. Discussion started: 15 July 2026

References

Abe-Ouchi, A., Saito, F., Kawamura, K., Raymo, M.E., Okuno, J., Takahashi, K., Blatter, H. Insolation-driven 100,000-year glacial cycles and hysteresis of ice-sheet volume. Nature 500, 190–193. https://doi.org/10.1038/nature12374, 2013.

Argus, D.F., Peltier, W.R., Drummond, R., Moore, A.W. The Antarctica component of postglacial rebound model ICE-6G_C (VM5a) based on GPS positioning, exposure age dating of ice thicknesses, and relative sea level histories. Geophys. J. Int. 198, 537–563. https://doi.org/10.1093/gji/ggu140, 2014.

Arthur, F., Roche, D.M., Fyfe, R., Quiquet, A., Renssen, H. Simulations of the Holocene Climate in Europe Using Dynamical Downscaling within the iLOVECLIM model (version 1.1). https://doi.org/10.5194/cp-2022-21, 2022.

Arthur, F., Zapolska, A., Roche, D.M., Li, H., Renssen, H. Modelling the Climate of the Eemian in Europe Using an Interactive Physical Downscaling. https://doi.org/10.20944/preprints202502.0262.v1, 2025.

Beghin, P., Charbit, S., Dumas, C., Kageyama, M., Roche, D.M., Ritz, C. Interdependence of the growth of the Northern Hemisphere ice sheets during the last glaciation: the role of atmospheric circulation. Clim. Past 10, 345–358. https://doi.org/10.5194/cp-10-345-2014, 2014.

Beghin, P., Charbit, S., Kageyama, M., Combourieu-Nebout, N., Hatté, C., Dumas, C., Peterschmitt, J.-Y. What drives LGM precipitation over the western Mediterranean? A study focused on the Iberian Peninsula and northern Morocco. Clim. Dyn. 46, 2611–2631. https://doi.org/10.1007/s00382-015-2720-0, 2016.

Berger, A.L. Long-Term Variations of Caloric Insolation Resulting from the Earth's Orbital Elements. Quat. Res. 9, 139–167. https://doi.org/10.1016/0033-5894(78)90064-9, 1978.

Bouttes, N., Lhardy, F., Quiquet, A., Paillard, D., Goosse, H., Roche, D.M. Deglacial climate changes as forced by different ice sheet reconstructions. Clim. Past 19, 1027–1042. https://doi.org/10.5194/cp-19-1027-2023, 2023.

Braconnot, P., Harrison, S.P., Kageyama, M., Bartlein, P.J., Masson-Delmotte, V., Abe-Ouchi, A., Otto-Bliesner, B., Zhao, Y. Evaluation of climate models using palaeoclimatic data. Nat. Clim. Change 2, 417–424. https://doi.org/10.1038/nclimate1456, 2012.

Brovkin, V., Ganopolski, A., Svirezhev, Y. A continuous climate-vegetation classification for use in climate-biosphere studies. Ecol. Model. 101, 251–261. https://doi.org/10.1016/S0304-3800(97)00049-5, 1997.

Calov, R., Ganopolski, A., Claussen, M., Petoukhov, V., Greve, R. Transient simulation of the last glacial inception. Part I: glacial inception as a bifurcation in the climate system. Clim. Dyn. 24, 545–561. https://doi.org/10.1007/s00382-005-0007-6, 2005.

Chandan, D., Peltier, W.R. Regional and global climate for the mid-Pliocene using the University of Toronto version of CCSM4 and PlioMIP2 boundary conditions. Clim. Past 13, 919–942. https://doi.org/10.5194/cp-13-919-2017, 2017.

Cheddadi, R., Fady, B., François, L., Hajar, L., Suc, J. -P., Huang, K., Demarteau, M., Vendramin, G.G., Ortu, E. Putative glacial refugia of *Cedrus atlantica* deduced from Quaternary pollen records and modern genetic diversity. J. Biogeogr. 36, 1361–1371. https://doi.org/10.1111/j.1365-2699.2008.02063.x, 2009.

Chevalier, M., Davis, B.A.S., Heiri, O., Seppä, H., Chase, B.M., Gajewski, K., Lacourse, T., Telford, R.J., Finsinger, W., Guiot, J., Kühl, N., Maezumi, S.Y., Tipton, J.R., Carter, V.A., Brussel, T., Phelps, L.N., Dawson, A., Zanon, M., Vallé, F., Nolan, C., Mauri, A., De Vernal, A., Izumi, K., Holmström, L., Marsicek, J., Goring, S., Sommer, P.S., Chaput, M., Kupriyanov, D. Pollen-based climate reconstruction techniques for late Quaternary studies. Earth-Sci. Rev. 210, 103384. https://doi.org/10.1016/j.earscirev.2020.103384, 2020.

Clark, P.U., Mix, A.C. Ice sheets and sea level of the Last Glacial Maximum. https://doi.org/10.1016/S0277-3791(01)00118-4, 2001.

Deser, C., Walsh, J.E., Timlin, M.S. Arctic Sea Ice Variability in the Context of Recent Atmospheric Circulation Trends. J. Clim. 13, 617–633. https://doi.org/10.1175/1520-0442(2000)013%3C0617:ASIVIT%3E2.0.CO;2, 2000.

Duprat-Oualid, F., Rius, D., Bégeot, C., Magny, M., Millet, L., Wulf, S., Appelt, O. Vegetation response to abrupt climate changes in Western Europe from 45 to 14.7k cal a BP: the Bergsee lacustrine record (Black Forest, Germany). J. Quat. Sci. 32, 1008–1021. https://doi.org/10.1002/jqs.2972, 2017.

Fénisse, G., Chevalier, M., Peyron, O., Bekaert, D. V., and Blard, P.-H.: Advancing Last Glacial Maximum paleoclimate reconstructions in Europe using pollen data: a multi-method (mega)biomization approach, EGUsphere [preprint], https://doi.org/10.5194/egusphere-2026-1590, 2026.

Gent, P.R., Danabasoglu, G., Donner, L.J., Holland, M.M., Hunke, E.C., Jayne, S.R., Lawrence, D.M., Neale, R.B., Rasch, P.J., Vertenstein, M., Worley, P.H., Yang, Z.-L., Zhang, M. The Community Climate System Model Version 4. J. Clim. 24, 4973–4991. https://doi.org/10.1175/2011JCLI4083.1, 2011.

Giorgetta, M.A., Jungclaus, J., Reick, C.H., Legutke, S., Bader, J., Böttinger, M., Brovkin, V., Crueger, T., Esch, M., Fieg, K., Glushak, K., Gayler, V., Haak, H., Hollweg, H., Ilyina, T., Kinne, S., Kornblueh, L., Matei, D., Mauritsen, T., Mikolajewicz, U., Mueller, W., Notz, D., Pithan, F., Raddatz, T., Rast, S., Redler, R., Roeckner, E., Schmidt, H., Schnur, R., Segschneider, J., Six, K.D., Stockhause, M., Timmreck, C., Wegner, J., Widmann, H., Wieners, K., Claussen, M., Marotzke, J., Stevens, B. Climate and carbon cycle changes from 1850 to 2100 in MPI-ESM simulations for the Coupled Model Intercomparison Project phase 5. J. Adv. Model. Earth Syst. 5, 572–597. https://doi.org/10.1002/jame.20038, 2013.

Goelzer, H., Huybrechts, P., Loutre, M.-F., Fichefet, T. Last Interglacial climate and sea-level evolution from a coupled ice sheet–climate model. Clim. Past 12, 2195–2213. https://doi.org/10.5194/cp-12-2195-2016, 2016.

Goosse, H., Brovkin, V., Fichefet, T., Haarsma, R., Huybrechts, P., Jongma, J., Mouchet, A., Selten, F., Barriat, P.-Y., Campin, J.-M., Deleersnijder, E., Driesschaert, E., Goelzer, H., Janssens, I., Loutre, M.-F., Morales Maqueda, M.A., Opsteegh, T., Mathieu, P.-P., Munhoven, G., Pettersson, E.J., Renssen, H., Roche, D.M., Schaeffer, M., Tartinville, B., Timmermann, A., Weber, S.L. Description of the Earth system model of intermediate complexity LOVECLIM version 1.2. Geosci. Model Dev. 3, 603–633. https://doi.org/10.5194/gmd-3-603-2010, 2010.

https://doi.org/10.5194/egusphere-2026-3988
Preprint. Discussion started: 15 July 2026

Guiot, J., Pons, A., De Beaulieu, J.L., Reille, M. A 140,000-year continental climate reconstruction from two European pollen records. Nature 338, 309–313. https://doi.org/10.1038/338309a0, 1989.

Hajima, T., Watanabe, M., Yamamoto, A., Tatebe, H., Noguchi, M.A., Abe, M., Ohgaito, R., Ito, Akinori, Yamazaki, D., Okajima, H., Ito, Akihiko, Takata, K., Ogochi, K., Watanabe, S., Kawamiya, M. Development of the MIROC-ES2L Earth system model and the evaluation of biogeochemical processes and feedbacks. Geosci. Model Dev. 13, 2197–2244. https://doi.org/10.5194/gmd-13-2197-2020, 2020.

Hansen, J., Lacis, A., Rind, D., Russell, G., Stone, P., Fung, I., Ruedy, R., Lerner, J. Climate sensitivity: Analysis of feedback mechanisms, in: Hansen, J.E., Takahashi, T. (Eds.), Geophysical Monograph Series. American Geophysical Union, Washington, D. C., pp. 130–163. https://doi.org/10.1029/GM029p0130, 1984.

Harmand, D., Durand, M. Les glaciations dans les Vosges, in: Le Bassin Parisien : Un Nouveau Regard Sur La Géologie, Gély, Jean-Pierre; Hanot, Franck; Association Des Géologues Du Bassin Parisien. https://doi.org/978-2-9550042-0-3.%20(hal-01720506), 2014.

Harrison, S.P., Bartlein, P.J., Izumi, K., Li, G., Annan, J., Hargreaves, J., Braconnot, P., Kageyama, M. Evaluation of CMIP5 palaeo-simulations to improve climate projections. Nat. Clim. Change 5, 735–743. https://doi.org/10.5194/sp-5-opsr-17-2025, 2015.

Hernandez, F., Garcia Sotillo, M., Melet, A., 2024. A description of Model Intercomparison Processes and Techniques for Ocean Forecasting. https://doi.org/10.5194/sp-2024-39, 2015.

Heyman, B.M., Heyman, J., Fickert, T., Harbor, J.M. Paleo-climate of the central European uplands during the last glacial maximum based on glacier mass-balance modeling. Quat. Res. 79, 49–54. https://doi.org/10.1016/j.yqres.2012.09.005, 2013.

Hoar, M.R., Palutikof, J.P., Thorne, M.C. Model intercomparison for the present day, the mid-Holocene, and the Last Glacial Maximum over western Europe. J. Geophys. Res. Atmospheres 109, 2003JD004161. https://doi.org/10.1029/2003JD004161, 2004.

Izumi, K., Bartlein, P.J., Harrison, S.P. Consistent large-scale temperature responses in warm and cold climates. Geophys. Res. Lett. 40, 1817–1823. https://doi.org/10.1002/grl.50350, 2013.

Jahn, A., Claussen, M., Ganopolski, A., Brovkin, V. Quantifying the effect of vegetation dynamics on the climate of the Last Glacial Maximum. Clim. Past., 1, 1–7, https://doi.org/10.5194/cp-1-1-2005, 2005.

Joussaume, S., Taylor, K., 1995. Status of the paleoclimate modeling intercomparison project. Proc. First Int. AMIP Sci. Conf. 425–430, https://doi.org/10.5194/cp-1-1-2005, 2005.

Joussaume, S., Taylor, K.E., Braconnot, P., Mitchell, J.F.B., Kutzbach, J.E., Harrison, S.P., Prentice, I.C., Broccoli, A.J., Abe-Ouchi, A., Bartlein, P.J., Bonfils, C., Dong, B., Guiot, J., Herterich, K., Hewitt, C.D., Jolly, D., Kim, J.W., Kislov, A., Kitoh, A., Loutre, M.F., Masson, V., McAvaney, B., McFarlane, N., De Noblet, N., Peltier, W.R., Peterschmitt, J.Y., Pollard, D., Rind, D., Royer, J.F., Schlesinger, M.E., Syktus, J., Thompson, S., Valdes, P., Vettoretti, G., Webb, R.S., Wyputta, U. Monsoon changes for 6000 years ago: Results of 18 simulations from the Paleoclimate Modeling Intercomparison Project (PMIP). Geophys. Res. Lett. 26, 859–862. https://doi.org/10.1029/1999GL900126, 1999.

https://doi.org/10.5194/egusphere-2026-3988
Preprint. Discussion started: 15 July 2026

Kageyama, M., D'Andrea, F., Ramstein, G., Valdes, P.J., Vautard, R. Weather regimes in past climate atmospheric general circulation model simulations. Clim. Dyn. 15, 773–793. https://doi.org/10.1007/s003820050315, 1999.

Kageyama, M., Albani, S., Braconnot, P., Harrison, S.P., Hopcroft, P.O., Ivanovic, R.F., Lambert, F., Marti, O., Peltier, W.R., Peterschmitt, J.-Y., Roche, D.M., Tarasov, L., Zhang, Xu, Brady, E.C., Haywood, A.M., LeGrande, A.N., Lunt, D.J., Mahowald, N.M., Mikolajewicz, U., Nisancioglu, K.H., Otto-Bliesner, B.L., Renssen, H., Tomas, R.A., Zhang, Q., Abe-Ouchi, A., Bartlein, P.J., Cao, J., Li, Q., Lohmann, G., Ohgaito, R., Shi, X., Volodin, E., Yoshida, K., Zhang, Xiao, Zheng, W. The PMIP4 contribution to CMIP6 – Part 4: Scientific objectives and experimental design of the PMIP4-CMIP6 Last Glacial Maximum experiments and PMIP4 sensitivity experiments. Geosci. Model Dev. 10, 4035–4055. https://doi.org/10.5194/gmd-10-4035-2017, 2017.

Kageyama, M., Braconnot, P., Harrison, S.P., Haywood, A.M., Jungclaus, J.H., Otto-Bliesner, B.L., Peterschmitt, J.-Y., Abe-Ouchi, A., Albani, S., Bartlein, P.J., Brierley, C., Crucifix, M., Dolan, A., Fernandez-Donado, L., Fischer, H., Hopcroft, P.O., Ivanovic, R.F., Lambert, F., Lunt, D.J., Mahowald, N.M., Peltier, W.R., Phipps, S.J., Roche, D.M., Schmidt, G.A., Tarasov, L., Valdes, P.J., Zhang, Q., Zhou, T. The PMIP4 contribution to CMIP6 – Part 1: Overview and over-arching analysis plan. Geosci. Model Dev. 11, 1033–1057. https://doi.org/10.5194/gmd-11-1033-2018, 2018.

Kageyama, M., Harrison, S.P., Kapsch, M.-L., Lofverstrom, M., Lora, J.M., Mikolajewicz, U., Sherriff-Tadano, S., Vadsaria, T., Abe-Ouchi, A., Bouttes, N., Chandan, D., Gregoire, L.J., Ivanovic, R.F., Izumi, K., LeGrande, A.N., Lhardy, F., Lohmann, G., Morozova, P.A., Ohgaito, R., Paul, A., Peltier, W.R., Poulsen, C.J., Quiquet, A., Roche, D.M., Shi, X., Tierney, J.E., Valdes, P.J., Volodin, E., Zhu, J. The PMIP4 Last Glacial Maximum experiments: preliminary results and comparison with the PMIP3 simulations. Clim. Past 17, 1065–1089. https://doi.org/10.5194/cp-17-1065-2021, 2021.

Laîné, A., Kageyama, M., Salas-Mélia, D., Voldoire, A., Rivière, G., Ramstein, G., Planton, S., Tyteca, S., Peterschmitt, J.Y. Northern hemisphere storm tracks during the last glacial maximum in the PMIP2 ocean-atmosphere coupled models: energetic study, seasonal cycle, precipitation. Clim. Dyn. 32, 593–614. https://doi.org/10.1007/s00382-008-0391-9, 2009.

Lamarque, J.-F., Shindell, D.T., Josse, B., Young, P.J., Cionni, I., Eyring, V., Bergmann, D., Cameron-Smith, P., Collins, W.J., Doherty, R., Dalsoren, S., Faluvegi, G., Folberth, G., Ghan, S.J., Horowitz, L.W., Lee, Y.H., MacKenzie, I.A., Nagashima, T., Naik, V., Plummer, D., Righi, M., Rumbold, S.T., Schulz, M., Skeie, R.B., Stevenson, D.S., Strode, S., Sudo, K., Szopa, S., Voulgarakis, A., Zeng, G. The Atmospheric Chemistry and Climate Model Intercomparison Project (ACCMIP): overview and description of models, simulations and climate diagnostics. Geosci. Model Dev. 6, 179–206. https://doi.org/10.5194/gmd-6-179-2013, 2013.

Lhardy, F., Bouttes, N., Roche, D.M., Crosta, X., Waelbroeck, C., Paillard, D. Impact of Southern Ocean surface conditions on deep ocean circulation during the LGM: a model analysis. Clim. Past 17, 1139–1159. https://doi.org/10.5194/cp-17-1139-2021, 2021.

Li, C., Battisti, D.S. Reduced Atlantic Storminess during Last Glacial Maximum: Evidence from a Coupled Climate Model. J. Clim. 21, 3561–3579. https://doi.org/10.1175/2007JCLI2166.1, 2008.

Lofverstrom, M., Liakka, J. The influence of atmospheric grid resolution in a climate model-forced ice sheet simulation. The Cryosphere 12, 1499–1510. https://doi.org/10.5194/tc-12-1499-2018, 2018.

Masson-Delmotte, V., Kageyama, M., Braconnot, P., Charbit, S., Krinner, G., Ritz, C., Guilyardi, E., Jouzel, J., Abe-Ouchi, A., Crucifix, M., Gladstone, R.M., Hewitt, C.D., Kitoh, A., LeGrande, A.N.,

https://doi.org/10.5194/egusphere-2026-3988
Preprint. Discussion started: 15 July 2026

Marti, O., Merkel, U., Motoi, T., Ohgaito, R., Otto-Bliesner, B., Peltier, W.R., Ross, I., Valdes, P.J., Vettoretti, G., Weber, S.L., Wolk, F., Yu, Y. Past and future polar amplification of climate change: climate model intercomparisons and ice-core constraints. Clim. Dyn. 26, 513–529. https://doi.org/10.1007/s00382-005-0081-9, 2006.

Mauritsen, T., Bader, J., Becker, T., Behrens, J., Bittner, M., Brokopf, R., Brovkin, V., Claussen, M., Crueger, T., Esch, M., Fast, I., Fiedler, S., Fläschner, D., Gayler, V., Giorgetta, M., Goll, D.S., Haak, H., Hagemann, S., Hedemann, C., Hohenegger, C., Ilyina, T., Jahns, T., Jimenéz-de-la-Cuesta, D., Jungclaus, J., Kleinen, T., Kloster, S., Kracher, D., Kinne, S., Kleberg, D., Lasslop, G., Kornblueh, L., Marotzke, J., Matei, D., Meraner, K., Mikolajewicz, U., Modali, K., Möbis, B., Müller, W.A., Nabel, J.E.M.S., Nam, C.C.W., Notz, D., Nyawira, S., Paulsen, H., Peters, K., Pincus, R., Pohlmann, H., Pongratz, J., Popp, M., Raddatz, T.J., Rast, S., Redler, R., Reick, C.H., Rohrschneider, T., Schemann, V., Schmidt, H., Schnur, R., Schulzweida, U., Six, K.D., Stein, L., Stemmler, I., Stevens, B., Von Storch, J., Tian, F., Voigt, A., Vrese, P., Wieners, K., Wilkenskjeld, S., Winkler, A., Roeckner, E. Developments in the MPI-M Earth System Model version 1.2 (MPI-ESM1.2) and Its Response to Increasing CO_2. J. Adv. Model. Earth Syst. 11, 998–1038. https://doi.org/10.1029/2018MS001400, 2019.

Morgan, J.D., Buizert, C., Fudge, T.J., Kawamura, K., Severinghaus, J.P., Trudinger, C.M. Gas isotope thermometry in the South Pole and Dome Fuji ice cores provides evidence for seasonal rectification of ice core gas records. The Cryosphere 16, 2947–2966. https://doi.org/10.5194/tc-16-2947-2022, 2022.

Ohgaito, R., Yamamoto, A., Hajima, T., O'ishi, R., Abe, M., Tatebe, H., Abe-Ouchi, A., Kawamiya, M. PMIP4 experiments using MIROC-ES2L Earth system model. Geosci. Model Dev. 14, 1195–1217. https://doi.org/10.5194/gmd-14-1195-2021, 2021.

Opsteegh, J.D., Haarsma, R.J., Selten, F.M., Kattenberg, A. ECBILT: a dynamic alternative to mixed boundary conditions in ocean models. Tellus A 50, 348–367. https://doi.org/10.1034/j.1600-0870.1998.t01-1-00007.x, 1998.

Orbe, C., Rind, D., Miller, R.L., Nazarenko, L.S., Romanou, A., Jonas, J., Russell, G.L., Kelley, M., Schmidt, G.A. Atmospheric Response to a Collapse of the North Atlantic Circulation under a Mid-Range Future Climate Scenario: A Regime Shift in Northern Hemisphere Dynamics. J. Clim. 36, 6669–6693. https://doi.org/10.1175/JCLI-D-22-0841.1, 2023.

Otto-Bliesner, B.L., Joussaume, S., Braconnot, P., Harrison, S.P., Abe-Ouchi, A. Modeling and Data Syntheses of Past Climates: Paleoclimate Modelling Intercomparison Project Phase II Workshop; Estes Park, Colorado, 15–19 September 2008. Eos Trans. Am. Geophys. Union 90, 93–93. https://doi.org/10.1029/2009EO110013, 2009.

Pausata, F.S.R., Li, C., Wettstein, J.J., Nisancioglu, K.H., Battisti, D.S. Changes in atmospheric variability in a glacial climate and the impacts on proxy data: a model intercomparison. Clim Past, https://doi.org/10.5194/cp-5-489-2009, 2009.

Pausata, F.S.R., Li, C., Wettstein, J.J., Kageyama, M., Nisancioglu, K.H. The key role of topography in altering North Atlantic atmospheric circulation during the last glacial period. Clim. Past 7, 1089–1101. https://doi.org/10.5194/cp-7-1089-2011, 2011.

Peltier, W.R. GLOBAL GLACIAL ISOSTASY AND THE SURFACE OF THE ICE-AGE EARTH: The ICE-5G (VM2) Model and GRACE. Annu. Rev. Earth Planet. Sci. 32, 111–149. https://doi.org/10.1146/annurev.earth.32.082503.144359, 2004.

https://doi.org/10.5194/egusphere-2026-3988
Preprint. Discussion started: 15 July 2026

Peltier, W.R., Argus, D.F., Drummond, R. Space geodesy constrains ice age terminal deglaciation: The global ICE-6G_C (VM5a) model. J. Geophys. Res. Solid Earth 120, 450–487. https://doi.org/10.1002/2014JB011176, 2015.

Peltier, W.R., Vettoretti, G. Dansgaard-Oeschger oscillations predicted in a comprehensive model of glacial climate: A "kicked" salt oscillator in the Atlantic. Geophys. Res. Lett. 41, 7306–7313. https://doi.org/10.1002/2014GL061413, 2014.

Peyron, O., Guiot, J., Cheddadi, R., Tarasov, P., Reille, M., De Beaulieu, J.-L., Bottema, S., Andrieu, V. Climatic Reconstruction in Europe for 18,000 YR B.P. from Pollen Data. Quat. Res. 49, 183–196. https://doi.org/10.1006/qres.1997.1961, 1998.

Quiquet, A., Dumas, C., Ritz, C., Peyaud, V., Roche, D.M. The GRISLI ice sheet model (version 2.0): calibration and validation for multi-millennial changes of the Antarctic ice sheet. Geosci. Model Dev. 11, 5003–5025. https://doi.org/10.5194/gmd-11-5003-2018, 2018.

Ramstein, G., Kageyama, M., Guiot, J., Wu, H., Hely, C., Krinner, G., Brewer, S. How cold was Europe at the Last Glacial Maximum? A synthesis of the progress achieved since the first PMIP model-data comparison. Clim Past. https://doi.org/10.5194/cp-3-331-2007, 2007.

Reeh, N. Parameterization of Melt Rate and Surface Temperature on the Greenland Ice Sheet, *Polarforschung 5913:* 113-128, 1991.

Rehfeld, K., Trachsel, M., Telford, R.J., Laepple, T. Assessing performance and seasonal bias of pollen-based climate reconstructions in a perfect model world. Clim. Past 12, 2255–2270. https://doi.org/10.5194/cp-12-2255-2016, 2016.

Renssen, H., Seppä, H., Heiri, O., Roche, D.M., Goosse, H., Fichefet, T. The spatial and temporal complexity of the Holocene thermal maximum. Nat. Geosci. 2, 411–414. https://doi.org/10.1038/ngeo513, 2009.

Robles, M., Peyron, O., Ménot, G., Brugiapaglia, E., Wulf, S., Appelt, O., Blache, M., Vannière, B., Dugerdil, L., Paura, B., Ansanay-Alex, S., Cromartie, A., Charlet, L., Guédron, S., De Beaulieu, J.-L., Joannin, S. Climate changes during the Late Glacial in southern Europe: new insights based on pollen and brGDGTs of Lake Matese in Italy. Clim. Past 19, 493–515. https://doi.org/10.5194/cp-19-493-2023, 2023.

Roche, D.M., Dumas, C., Bügelmayer, M., Charbit, S., Ritz, C. Adding a dynamical cryosphere to *i* LOVECLIM (version 1.0): coupling with the GRISLI ice-sheet model. Geosci. Model Dev. 7, 1377–1394. https://doi.org/10.5194/gmd-7-1377-2014, 2014.

Rørvik, K.-L., Laberg, J.S., Hald, M., Ravna, E.K., Vorren, T.O. Behavior of the northwestern part of the Fennoscandian Ice Sheet during the Last Glacial Maximum – a response to external forcing. Quat. Sci. Rev. 29, 2224–2237. https://doi.org/10.1016/j.quascirev.2010.05.022, 2010.

Russo, E., Buzan, J., Lienert, S., Jouvet, G., Velasquez Alvarez, P., Davis, B., Ludwig, P., Joos, F., Raible, C.C. High-resolution LGM climate of Europe and the Alpine region using the regional climate model WRF. Clim. Past 20, 449–465. https://doi.org/10.5194/cp-20-449-2024, 2024.

Schlosser, E., Oerter, H. Seasonal variations of accumulation and the isotope record in ice cores: a study with surface snow samples and firn cores from Neumayer station, Antarctica. Ann. Glaciol. 35, 97–101. https://doi.org/10.3189/172756402781817374, 2002.

https://doi.org/10.5194/egusphere-2026-3988
Preprint. Discussion started: 15 July 2026

Seguinot, J., Ivy-Ochs, S., Jouvet, G., Huss, M., Funk, M., Preusser, F. Modelling last glacial cycle ice dynamics in the Alps. The Cryosphere 12, 3265–3285. https://doi.org/10.5194/tc-12-3265-2018, 2018.

Sepulchre, P., Caubel, A., Ladant, J.-B., Bopp, L., Boucher, O., Braconnot, P., Brockmann, P., Cozic, A., Donnadieu, Y., Dufresne, J.-L., Estella-Perez, V., Ethé, C., Fluteau, F., Foujols, M.-A., Gastineau, G., Ghattas, J., Hauglustaine, D., Hourdin, F., Kageyama, M., Khodri, M., Marti, O., Meurdesoif, Y., Mignot, J., Sarr, A.-C., Servonnat, J., Swingedouw, D., Szopa, S., Tardif, D. IPSL-CM5A2 – an Earth system model designed for multi-millennial climate simulations. Geosci. Model Dev. 13, 3011–3053. https://doi.org/10.5194/gmd-13-3011-2020, 2020.

Sidorenko, D., Rackow, T., Jung, T., Semmler, T., Barbi, D., Danilov, S., Dethloff, K., Dorn, W., Fieg, K., Goessling, H.F., Handorf, D., Harig, S., Hiller, W., Juricke, S., Losch, M., Schröter, J., Sein, D.V., Wang, Q. Towards multi-resolution global climate modeling with ECHAM6–FESOM. Part I: model formulation and mean climate. Clim. Dyn. 44, 757–780. https://doi.org/10.1007/s00382-014-2290-6, 2015.

Tierney, J.E., Zhu, J., King, J., Malevich, S.B., Hakim, G.J., Poulsen, C.J. Glacial cooling and climate sensitivity revisited. Nature 584, 569–573. https://doi.org/10.1038/s41586-020-2617-x, 2020.

Timm, O., Timmermann, A. Simulation of the Last 21 000 Years Using Accelerated Transient Boundary Conditions*. J. Clim. 20, 4377–4401. https://doi.org/10.1175/JCLI4237.1, 2007.

Ullman, D.J., LeGrande, A.N., Carlson, A.E., Anslow, F.S., Licciardi, J.M. Assessing the impact of Laurentide Ice Sheet topography on glacial climate. Clim. Past 10, 487–507. https://doi.org/10.5194/cp-10-487-2014, 2014.

Valdes, P.J., Armstrong, E., Badger, M.P.S., Bradshaw, C.D., Bragg, F., Crucifix, M., Davies-Barnard, T., Day, J.J., Farnsworth, A., Gordon, C., Hopcroft, P.O., Kennedy, A.T., Lord, N.S., Lunt, D.J., Marzocchi, A., Parry, L.M., Pope, V., Roberts, W.H.G., Stone, E.J., Tourte, G.J.L., Williams, J.H.T. The BRIDGE HadCM3 family of climate models: HadCM3@Bristol v1.0. Geosci. Model Dev. 10, 3715–3743. https://doi.org/10.5194/gmd-10-3715-2017, 2017.

Volodin, Evgeny; Mortikov, Evgeny; Gritsun, Andrey; Lykossov, Vasily; Galin, Vener; Diansky, Nikolay; Gusev, Anatoly; Kostrykin, Sergey; Iakovlev, Nikolay; Shestakova, Anna; Emelina, Svetlana (2023). IPCC DDC: INM INM-CM4-8 model output prepared for CMIP6 CMIP. World Data Center for Climate (WDCC) at DKRZ. https://doi.org/10.26050/WDCC/AR6.C6CMINIC8, 2023.

Yukimoto, S., Adachi, Y., Hosaka, M., Sakami, T., Yoshimura, H., Hirabara, M., Tanaka, T.Y., Shindo, E., Tsujino, H., Deushi, M., Mizuta, R., Yabu, S., Obata, A., Nakano, H., Koshiro, T., Ose, T., Kitoh, A. A New Global Climate Model of the Meteorological Research Institute: MRI-CGCM3 —Model Description and Basic Performance—. J. Meteorol. Soc. Jpn. Ser II 90A, 23–64. https://doi.org/10.2151/jmsj.2012-A02, 2012.

Zheng, W., Zhang, Z., Chen, L., Yu, Y. The mid-Pliocene climate simulated by FGOALS-g2. Geosci. Model Dev. 6, 1127–1135. https://doi.org/10.5194/gmd-6-1127-2013, 2013.

Zhu, J., Otto-Bliesner, B.L., Brady, E.C., Gettelman, A., Bacmeister, J.T., Neale, R.B., Poulsen, C.J., Shaw, J.K., McGraw, Z.S., Kay, J.E. LGM Paleoclimate Constraints Inform Cloud Parameterizations and Equilibrium Climate Sensitivity in CESM2. J. Adv. Model. Earth Syst. 14, e2021MS002776. https://doi.org/10.1029/2021MS002776, 2022.